LDACS1 Navigation Performance Assessment By Flight Trials

Nicolas Schneckenburger, Bernard P. B. Elwischger, Boubeker Belabbas, Dmitriy Shutin,
Mihaela-Simona Circiu, Matthias Suess, Michael Schnell, Johann Furthner, and Michael Meurer
German Aerospace Center (DLR)
Institute of Communications and Navigation
Oberpfaffenhofen, 82234 Wessling, Germany
mail: nicolas.schneckenburger@dlr.de

***Abstract*—The presented paper discusses the validation of a new aeronautical communication system LDACS1 for navigation to implement an alternative positioning, navigation, and timing service. To this end, a flight measurement campaign has been prepared and realized in November 2012. The measurement setup includes four ground stations transmitting an LDACS1 signal, and a single airborne receiver placed in Falcon 20E aircraft. To mitigate the clock related errors, the station clocks are synchronized using GPS time transfer.**

The paper outlines the measurement campaign. To assess the performance of the ranging, preliminary snapshot based results are evaluated in terms of their accuracy. Also, a 2D position solution is calculated with the altitude information taken from a simulated barometer. The obtained results for the analyzed flight segment show a root mean squared error for the 2D position below 15 m.

BIOGRAPHIES

Nicolas Schneckenburger received his Dipl.-Ing. (M.Sc) degree in electrical engineering from the University of Ulm, Germany, in 2010. Since then he has been working as a research associate with the Institute of Communications and Navigation at the German Aerospace Center (DLR). His main focus in the last years has been on new communication systems in civil aviation and their utilization for navigation.

Bernard P. B. Elwischger received his Dipl.-Ing. (M.Sc) degree in electrical engineering from Vienna University of Technology, Austria. He was a research assistant at the Institute of Integrated Sensor Systems of the Austrian Academy of Sciences, and wrote his master thesis about the efficiency of positioning algorithms. Currently, he works at DLR in the fields of navigation and synchronization in positioning and timing systems, in particular GNSS.

Boubeker Belabbas is the leader of the integrity group of the Institute of Communications and Navigation at the DLR. He obtained an M.Sc degree in mechanical engineering from the Ecole Nationale Supérieure de lElectricité et de Mecanique in Nancy, France, and a specialized M.Sc in aerospace mechanics from Ecole Nationale Supérieure de lAéronautique et de l'Espace in Toulouse, France.

Dmitriy Shutin received the Ph.D. degree in electrical engineering from Graz University of Technology (TUG), Austria, in 2006. During 2006-2009 he was an assistant professor at the Signal Processing and Speech Communication Laboratory at TUG. From 2009 to 2011 he was a research associate with the Department of Electrical Engineering at Princeton University, USA. Since 2011 he is with the German Aerospace Center. In 2009 he was awarded the Erwin Schroedinger Research Fellowship. He is Senior IEEE Member.

Mihaela-Simona Circiu studied computer engineering at the Technical University Gheorghe Asachi, Romania, where she wrote her master thesis on multi-objective genetic algorithms. She obtained in 2012 a 2nd level specialized M.Sc in navigation and related application from Politecnico di Torino, Italy. Currently, she works in the untegrity group at DLR.

Matthias Suess is member of the GNSS systems group of the Institute of Communications and Navigation at DLR. His research focuses on mathematical models of atomic clocks, robust steering and composite clock algorithms using modified Kalman filters. In 2009, he experienced a research visit at the U.S. Naval Observatory to study GNSS timing performances. He graduated as computer scientist with field of specialization in mathematical modelling at the University of Passau, Germany.

Michael Schnell received a Dipl.-Ing. (M.Sc) and a Ph.D. degree in electrical engineering in 1987 and 1997, respectively. Since 1990 he is scientific researcher at the Institute of Communications and Navigation at DLR where he is currently group leader of the Aeronautical Communications Group. Michael Schnell is Lecturer for multi-carrier communications at the University of Karlsruhe, Germany, and acts as selected Advisor for the German ATC Provider (DFS) within the Aeronautical Communications Panel of ICAO. He is Senior Member IEEE and member of VDE/ITG.

Johann Furthner received a Ph.D. in Physics in the field of laser physics at the University of Regensburg, Germany, in 1994. Since 1995 he is scientific staff at German Aerospace Centre (DLR). In 2008 he stayed half year at ESA in the Galileo Project Team. He is working on the development of navigation systems in a number

of areas. Since 2011 he is leader of the GNSS group at the Department of Navigation.

Michael Meurer is the head of the Department of Navigation at the DLR's Institute for Communications and Navigation, and the coordinating director of the DLR Centre of Excellence for Satellite Navigation. Since 2005 he has been an associate professor (PD) at the Technical University of Kaiserslautern. His current research interests include GNSS signals, GNSS receivers, interference mitigation and navigation for safety-critical applications.

I. Introduction

The rapid growth of civil air-traffic in the last decades has led to the necessity of a more efficient management of the airspace. This, however, is a very challenging task using the current communication, navigation and surveillance (CNS) infrastructure. A large number of mostly analog systems have either already reached their capacity limit or are expected to do so in the near future. Therefore, most systems in the civil aviation sector are currently undergoing a major modernization process.

As for communication aspects, the current analog voice radio system will have to be substituted by a more efficient one. This is both due to the lack of capacity of the legacy systems, as well as to the new performance requirements on the architecture. While in the past the communication between traffic controller and pilot used direct voice links, in the future the information will be exchanged using data links. One of the most promising candidates for the future air-traffic management (ATM) data link is the L-band digital aeronautical communication system type 1 (LDACS1). LDACS1 is largely based on 4th generation telecommunication technology and uses orthogonal frequency division multiplexing (OFDM) as modulation. Compared to the current analog systems, it offers a vastly increased capacity, scalability, and efficiency.

In the sector of aircraft navigation, currently also a paradigm shift is happening: In the past, pilots had to rely mainly on DME (distance measuring equipment) and VOR (VHF omnidirectional radio range). Compared to state-of-the-art navigation aids, e.g. GPS, these systems only offer a poor performance while being spectrally inefficient. Therefore, the aircraft will increasingly rely on GNSS (global navigation satellite systems) in the future, offering a highly superior navigation performance. To guarantee the required degree of integrity, the GNSS systems will be accompanied by a ground or satellite based augmentation system (G/SBAS).

An increased use of GNSS brings new challenges with regard to integrity, continuity and availability of the navigation information. Due to the low power levels received from distant satellites, navigation is susceptible to intentional or unintentional interference. Hence, a parallel navigational backup infrastructure less vulnerable against interference, referred to as alternative positioning, navigation and timing (APNT), needs to be employed. This system can be used when GNSS services are temporarily unavailable. As several past incidents show, e.g. the ones in Newark or South Korea, complete unavailability of GPS within a large area may not be a frequent, but still a real threat [1], [2].

Currently, the main approach for a backup system for GNSS relies on an increased use of DME technology. However, this exhibits different drawbacks: First of all, a costly extension of the infrastructure is required. Secondly, if the use of the spectrally inefficient DME system becomes intensified, additional spectral resources will be occupied. Thus, the deployment of the required new communication system in the L-band is obstructed. The necessary new communication infrastructure could not be implemented.

Therefore, the approach of using the future communication system LDACS1 for navigation is evaluated in this paper. As shown in [3], positioning with an OFDM system is generally possible with high accuracy. Navigation using LDACS1 has been proposed in [4], and in [5] the theoretic bounds for range estimation are assessed. It is shown that the regular LDACS1 transmit power is theoretically sufficient to offer high precision navigation within the cell service area. To verify these theoretical results and evaluate LDACS1's practical ability to act as an APNT system for GNSS backup, DLR has been planning a flight measurement campaign in 2011 and 2012. The flight mission was carried out in November 2012.

Currently, the initial evaluation of the measured data is being performed. This first analysis shows that, in most situations, LDACS1 offers a good navigation performance. Nevertheless challenges still exist: Multiple propagation paths (multipaths), as well as tropospheric errors turn out to cause degradation. Another challenge is the presence of interference by other onboard systems, like the DME.

In the following, we will begin with a brief description of the LDACS1 communication system. Next is a detailed description of the measurement campaign setup, including the specific challenges which had to be solved to conduct the campaign. It follows a description of the ground station synchronization concept, and the presentation of preliminary results for the range and position estimation. Therefore, a description and discussion of the employed algorithms is necessary. The paper concludes with a summary of the work, a discussion of open issues and an outlook on the future work to be conducted in the field of LDACS1 navigation.

II. LDACS1 communication system

The communication link from the ground station (GS) and to aircraft, here referred to as airborne station (AS), is denoted as forward link (FL). The FL signal is continuously transmitted and therefore offers a perfect opportunity for range measurements. LDACS1 is a cellular system, based on a network of synchronized ground stations. This enables positioning by determining ranges to multiple stations.

LDACS1 employs OFDM as modulation and shall be deployed in the aeronautical L-band (960-1164 MHz).

Each GS uses a 500 kHz channel. The OFDM DFT size is 64. Excluding guard bands, 50 sub-carriers can be used for transmission. Each OFDM symbol, consisting of a useful symbol duration of 102.4 µs (64 samples), is extended with a cyclic prefix (CP) of length 4.8 µs (3 samples). Additionally, a raised cosine windowing function is applied to each OFDM symbol, reducing its out-of-band radiation. This adds another 12.8 µs (8 samples) on each side of an OFDM symbol. Due to the overlapping of the windowing function between consecutive symbols, the overall symbol duration is 120 µs (75 samples). The overall CP and windowing overhead is thus about 15 %.

The largest entity in the FL signal is a super-frame (SF) with a duration of $t_{\mathrm{SF}} = 240$ ms. Each SF is composed of 2000 OFDM symbols. One SF consists of different types of sub-frames, dedicated to the transmission of different information from the GS to the AS. For more information on that topic, the reader is referred to the LDACS1 standard [6]. Table 1 summarizes the LDACS1 parameters.

Table 1: LDACS1 transmission parameters

Parameter	Value
Bandwidth	500 kHz
Nominal transmit power	39 dBm
DFT size	64
Subcarriers	50
Subcarrier spacing	≈ 9.7 kHz
Superframe (SF) length	240 ms
OFDM symbols in SF	2000
Sampling time	1.6 µs
Total symbol duration	120 µs
Windowing duration	12.8 µs
Cyclic prefix duration	4.8 µs

III. Measurement Campaign Setup

In this section, the planning and execution of the measurement campaign is described. This includes the different challenges which had to be solved, such as setting up of the hardware and the synchronization of the ground stations.

Two major goals for the measurement campaign can be identified:

1) Determination of the positioning accuracy using the LDACS1 communication signal
2) Validation of LDACS1 as a potential APNT candidate

This defines the key components on the entire setup:

- A system of four ground stations continuously transmits the LDACS1 FL signal. The stations are located in a geometry suitable for positioning, and are synchronized to nanosecond precision. The stations must have good visibility of the sky, i.e. must be located on open areas. Additionally the airspace over the stations must not be constrained by any safety regulations, e.g. a restricted area of a neighboring large airport or military facility.
- The receiving aircraft records the signals from the ground: To allow calculation for correct ranges to the station, the clock in the aircraft has to be monitored as well. The Falcon 20E, available for the campaign, is shown in Figure 1.
- Software to convert and analyze the recorded data, apply clock corrections and calculate the aircraft position.
- A procedure is required, which is able to precisely measure the positions of the different ground stations and the aircraft's positions during the flight.

Figure 1: Dassault Falcon 20E (D-CMET) employed in the measurement campaign.

A. Ground station setup

The four ground stations are located in the area south west of the DLR site in Oberpfaffenhofen and are shown in Figure 2. The exact positions and frequencies are given in Table 2. Station A is set up in a measurement van at the airport in Oberpfaffenhofen. Station B is erected on an open area next to a detached house near Marktoberdorf. Station C is installed at a small airport for general aviation pilots in Bad Wörishofen. The last station D is located on a

Table 2: GS positions and frequencies

Distance [km] from/ to	**A**	**B**	**C**	**D**
A - $f = 973.75$ MHz 48°5'8.91"N, 11°16'37.46"E	-	60	50	36
B - $f = 971.25$ MHz 47°45'5.53"N, 10°38'48.20"E	60	-	30	30
C - $f = 968.75$ MHz 48°0'58.99"N, 10°36'48.63"E	50	30	-	39
D - $f = 966.25$ MHz 47°50'4.57"N, 11°6'59.38"E	36	30	39	-

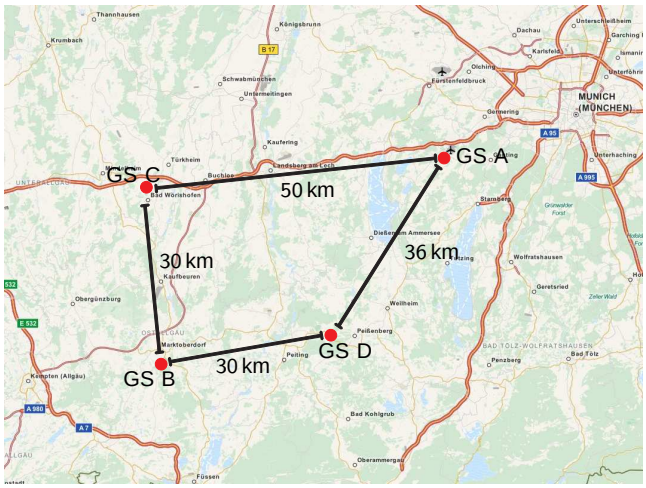

Figure 2: Ground station locations (©OpenStreetMap).

mountain next to a weather station near Peissenberg. The stations are between 60 and 30 km apart from each other. For its transmission, each GS uses a separate 500 kHz channel in the lower L-band between 965-975 MHz, as defined in Table 2 and Figure 3. There are no other users assigned to that band, the closest possible interferers are a TACAN station at the airport in Erding at 962 MHz and the GSM band below 960 MHz.

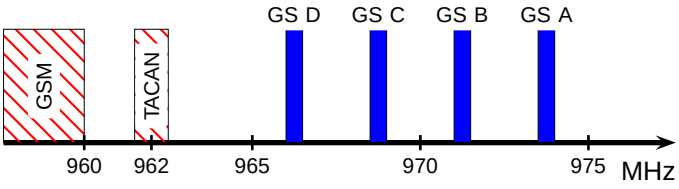

Figure 3: Frequencies of the stations and adjacent users.

The principal hardware configuration of a ground station is shown in Figure 4. Four main devices can be identified:

- A Rb (rubidium) atomic clock generates a 10 MHz clock signal for the signal generator and GPS receiver. The second output is a pulse-per-second (PPS) signal[1].
- The signal generator transmits the internally stored LDACS1 FL signal. The transmission is triggered by the PPS from the atomic clock. Each pulse initiates the transmission of four 240 ms SF. That means, in each second there is a 40 ms pause.
- A high power amplifier amplifies the output from the signal generator to an average transmit power of 39 dBm for transmission over an L-band aircraft antenna. The system contains two bandpass filters in order to reduce out of band radiation.

[1]At station A the rubidium clock was replaced by a caesium clock.

- The high precision multi-frequency GNSS receiver monitors the behavior of the atomic clock and logs its offset to the GPS master time. Hereby, it takes the PPS signal from the atomic clock and continuously makes measurements to the GPS time. Before the measurements, the receiver also determines the exact reference positions of the transmit antennas by long term measurements. These positions are required to calculate the aircraft's position from the measured LDACS1 pseudoranges.

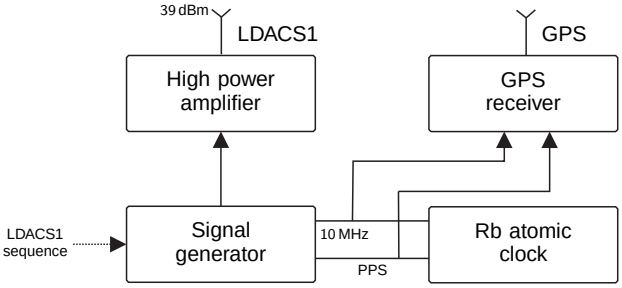

Figure 4: Schematic ground station hardware setup.

Using the setup above, the LDACS1 signal can be emitted at well defined times. The transmit times of all stations are referenced to the GPS time and therefore can be easily compared to each other.

B. Airborne station setup

The task of the hardware in the aircraft is to receive and record the signal emitted by the GS. The principal setup is shown in Figure 5. The aircraft measurement equipment consists of the following components:

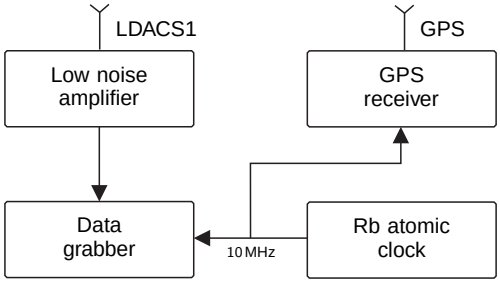

Figure 5: Airborne station hardware setup.

- A Rb atomic clock guarantees that all devices onboard are synchronized. To allow the determination of ranges between the aircraft and ground station A, station A is set up in a van. Thus, the exact offset of the atomic clocks in station A and the aircraft can be measured immediately before starting and after landing.
- The data grabber stores the received signal on a solid state disk and adds a timestamp with

a precision of $< 1\,\mu s$ to each record[2]. Using an internal FPGA, the received signal is digitally downconverted (DDC) and each channel stored separately in real time. The FPGA is also used for a real time analysis of the basic parameters, e.g. received spectrum and power levels. The data recording unit also includes a single-frequency GPS receiver which monitors the behavior of the atomic clock in the aircraft.

- A low noise amplifier amplifies the low powered signal received from the outside L-band antenna. The received signal is passed through several band-pass filters in order to reduce interference from adjacent frequency bands.
- High precision GPS receiver: The multi-frequency GPS receiver acts as reference system for the position measurements, i.e. the ranges calculated using LDACS1 are compared to those from that device.

The complete measurement configuration, including additional devices like the power supply equipment and monitoring computers, is divided up on three 19" racks and installed in the aircraft.

C. Error sources

Several error influences on both the position and range estimation exist. At this early stage a quantitative discussion of the errors is not yet possible. Nevertheless, different error influences may be identified qualitatively. A rigorous quantitative assessment of error influences is currently ongoing.

The synchronization of the ground stations plays a crucial role in the measurement setup. Therefore, inaccuracies of the clock synchronization may lead to a strong degradation of the position results and calibration.

Another source of errors are the internal transmission delays. As described above, a transmission of four SFs (each of length $240\,ms$) is initiated by a PPS pulse from the atomic clock. Although identical transmitter hardware is used in each station, they each exhibit a different time delay for the complete transmitter line, i.e. the signals are emitted at a slightly different time from each station. Although this delay is only in the order of 10ths of ns, it can result in range errors in the order of a few meters. This behavior is subject of current investigations. Note however, that this effect only becomes apparent for position and range measurements for station B,C, and D. For station A these delays are directly calibrated out.

An issue, which has to be investigated in the future, is the interference by onboard equipment. Compared to a DME pulse which is transmitted with a power of 1 kW, the power level of the LDACS1 signal received from the ground station is very low,e.g. as low as $-100\,dBm$. This significant difference in power leads to the DME emitting out of band radiation stronger than the received LDACS1 signal. Fortunately, the onboard DME only emits a little number of short pulses per second.

Another degradation of the performance is caused by the influences of the troposphere. Depending on air pressure and water concentration in the air, radio waves travel at different speeds. This has a direct effect on the estimated ranges. Although, models exist, they only partly apply, if the aircraft is seen under low elevation angles, i.e. on the horizon.

Minor influences include uncertainties about the antenna positions on the ground and at the aircraft. Even if mounted on solid tripods, small movements or inaccuracies of the antenna positions cannot be ruled out.

Adding to the errors above, there is always an uncertainty about the position measurements of the GPS reference system.

D. Execution of the campaign

The campaign was executed in November 2012. Before start and after landing, station A, mounted in a van, met the aircraft on the apron for clock synchronization. The pattern shown in Figure 6 was flown on three different altitudes, flight level 90 ($\approx 3000\,m$), 310 ($\approx 8500\,m$), and 390 ($\approx 11\,500\,m$). Hereby, the aircraft flew a 'butterfly' pattern over the stations, using each station as turning point. This allows the analysis of different real world geometric constellations. The entire flight took about $90\,min$.

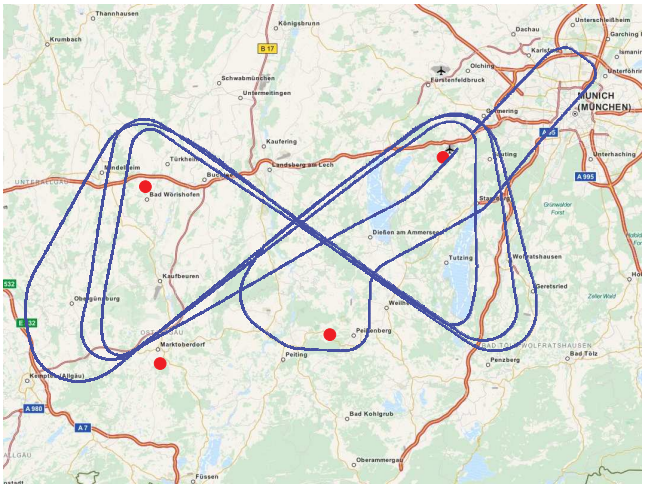

Figure 6: Route of the flight conducted on 13.11.2012 (©OpenStreetMap).

IV. Employed algorithms

In this section the employed algorithms, required for position estimation, are described. There are two prerequisites for the successful estimation of a position: Firstly, the pseudoranges between the stations and the receiver have to be known. These ranges still include an error due to the offset in the clock of the AS. The offset appears as an unknown variable in the equations and can be resolved during the calculation of the position.

[2]Compared to the maximum speed of the aircraft of $240\,m/s$ this value is negligible.

Note, that the geometry of the stations offer only a very poor vertical resolution. Thus positions are calculated horizontally, with the altitude information taken from the modelled barometer. The calculation of the positions can only work, if all ground station clocks are synchronized. Using rubidium clocks, which have an advanced short term stability, their offsets have to be known for every time instance.

A. Clock synchronization

Synchronization of the signals emitted by the four stations is achieved by providing each of the four signal generators a stable 10 Mhz stable reference signal as well as PPS signal. As shown in Figure 5, both signals are provided by the same oven-controlled rubidium clock, one being part of stations B, C, and D. In station A, a caesium clock is part of the station setup. In order to avoid decrease of the clock stability under varying environmental conditions, the clocks are housed in an additional oven-controlled chassis with shock-protection. The rubidium clocks are tuned by their deterministic drift values several days before the flight mission, and then let run freely. To keep them synchronized to each other, their time offsets and drifts are continuously monitored. This is achieved by referencing the atomic clocks of all stations individually to the atomic clocks from GPS satellites in view. In each station, the dual frequency GNSS timing receiver is set up to use the local atomic clock as reference, and conduct and continuously record code and phase measurements of all GPS signals in the L1 and L2 band at intervals of one second.
Based on those measurements, the time offsets of the atomic clocks are determined through application of a common view time transfer method. The method used for the results presented in this paper is similar to the modified Consultative Committee for Time and Frequency (CCTF) procedure proposed in [7]. It is code-based and uses the ionosphere-free combination P3. The carrier phase measurements are left unconsidered at this point, as the main point of interest is the determination of the absolute time delays, and not to maximize the frequency stability of the observations. However, it is planned to further investigate refinement of the actual time transfer method with techniques such as carrier smoothing and application of precise orbit products (e.g., from IGS).

The used synchronization approach requires calibration not only of all included cables, but the positions of the four GPS and and the four LDACS1 antennas as well. In order to determine the positions of the LDACS1 antennas, the GPS antennas were placed at the LDACS1 antenna mount points. By the aid of the GNSS timing receivers, data in Receiver Independent Exchange Format (RINEX) is recorded for several hours, so that the positions of the antennas can be determined straightforwardly through postprocessing. The calibration of the GPS antenna positions is achieved accordingly.
The calibration of the internal delays of the GNSS receivers is done with a GNSS hardware simulator. The applied calibration method is described in [8], and is based on prior calibration of the GNSS hardware simulator with a fast digital storage oscilloscope. Results from past calibration campaigns [9] and relative calibration experiments are taken into account to verify the absolute calibration results for the GNSS receivers used during the flight mission.

The accuracy of the synchronization achievable by the common-view time transfer technique depends on many factors, such as multipath effects on the GPS antennas, or atmospheric effects during the flight mission. A conservative estimation of the time accuracy achievable by this method can be given by 10 ns [10]. Assessment of the synchronization error distributions and final error budgets is still ongoing.

B. Calculation of ranges

If we are interested in a single range, knowledge of the offset between the involved clocks has to be present, i.e. the exact offset between the clock on ground and in air has to be known. With that knowledge, pseudoranges become ranges. Therefore, before the start of the aircraft and after landing, the offset is measured between the clocks in the aircraft and ground station A. Unfortunately, the drift of an atomic clock under the influence of vibrations or temperature and pressure changes, like the one experienced in the aircraft during flight, is usually not linear. Hence, a a second measurement, the Rb clock is roughly monitored using a single-frequency GPS receiver included in the data recorder. However, these measurements are prone to errors due to the high movement of the aircraft. Because of those reasons, some bias may still be present in the range measurements. Nevertheless, they can be seen as a good first performance indicator.

For the actual calculation of the ranges, all internal delays of transmitting and receiving hardware and cables, and filter characteristics have to be accounted for. While the determination of the individual influences would be an elaborate task, the sum of all influences can be easily calibrated out in one measurement. Therefore, the final and complete setup is arranged. In a transmitter-receiver calibration measurement, the antenna connector of the transmitter is directly connected to antenna input of the receiver. This measurement provides a zero distance calibration: Neglecting antennas delays, the receiver records the equivalent of a $0\,\mathrm{s}$ delay signal.

Using the calibration signal, the calculation of the pseudoranges is straightforward. One frame equals the distance of roughly $t_{\mathrm{SF}} \cdot c_0 \approx 100\,000\,\mathrm{km}$ (t_{SF}: duration of a super frame, c_0: speed of light). Therefore, a rough synchronization to the frame structure can be achieved by correlation with multiple symbols. This resolves ambiguities. To obtain the delay τ_{est} between the calibration data $c[k]$ and measurement data $m[k]$ the following function is minimized

$$\tau_{\mathrm{est}} = \underset{\tau}{\operatorname{argmin}} \ \mid m[k] - c[k-\tau] \mid^2 \tag{1}$$

It is well known that this problem may be solved by a correlation in the time domain [11]. Due to the $500\,\mathrm{kHz}$ bandwidth of the signal, the duration of a sample equals $480\,\mathrm{m}$. Therefore, interpolation has to be applied. For the results shown in this paper, FFT interpolation with an

oversampling factor of $r_{\text{up}} = 1024$ is applied. This results in one sample equaling 0.5 m which is sufficiently precise. Through multiplication by the speed of light in air, the pseudorange ρ is obtained.

C. Position determination

Let assume ρ_i being the pseudo range of a signal leaving the station i and received by the aircraft at a given epoch t. Let $P_{ECEF} = (x_1, x_2, x_3)$ being the unknown position of the aircraft in ECEF (Earth-Centered Earth-Fixed) coordinate system and b the aircraft clock offset to a common system time expressed in metesr. We also define the position in ENU (East North Up) coordinate system taking the initial guess P^0_{ECEF} as the reference, noted $P_{ENU|P^0_{ECEF}} = (x_e, x_n, x_u)$. The position and time state vector is considered as being $X = (x_e, x_n, x_{baro}, b)$, where x_{baro} is the vertical component of the position given by a barometric altimeter. During the flight trial, it would be able to calculate the vertical component of the position using LDACS1 and the barometric altimeter, but this would necessitate the use of one additional ranging source to solve the 4 D problem. LDACS1 is considered only for the estimation of the state subset (x_e, x_n, b). We assume that the initial guess of the position for the first epoch is given by the GPS position. As already mentioned, the initial position domain of convergence is beyond the scope of this paper. The barometric altimeter gives the altitude of the aircraft and the LDACS1 ranges are used to estimate the east and north components. For a given epoch, the searching algorithm is contained in the horizontal plan defined by $X = x_{baro}$.

The Newton-Raphson scheme is applied to define the best estimate of the horizontal position and the aircraft clock bias. The geometry matrix is a 4×3 matrix, where the first two columns represent the unit vectors from the projected stations (projected in the plan $X = x_{baro}$) to the position of the aircraft at a previous iteration. The third column of the geometry matrix is a column of ones (taking into consideration that the pseudo-ranges are acquired at the same time by the receiver on board of the aircraft).

After convergence to the best estimate of the aircraft position using LDACS1, the same algorithm is applied for all consecutive epochs, taking as initial point the best estimate of the position from the previous epoch.

V. Preliminary Results

In this section, preliminary results are shown. We begin with a part on the clock synchronization. Results for the calculated range between station A and the aircraft follow. The ranges from all stations are then later used to calculate the position of the aircraft.

A. Time transfer performance

The time transfer during the flight mission is conducted continuously in intervals of one second for all four stations, without any interruption. There are no outliers. Figure 7 shows the overlapping Allan deviation of all four station clocks observed by the used time transfer approach (please refer to section IV-A) during the flight mission.

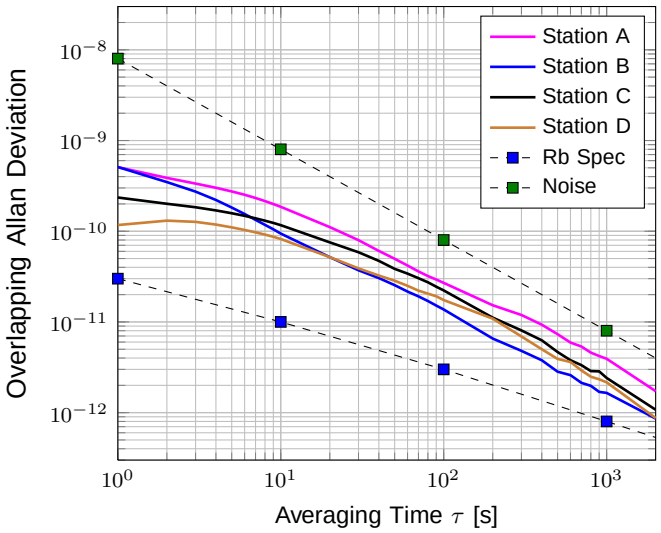

Figure 7: Observed Allan deviation of the rubidium clocks in the ground stations.

It should be mentioned that the observed time stabilities basically represent measurement noise, not clock instabilities. To distinguish the stability contribution from the observation noise and the clock itself, a conservative upper bound of the white observation noise is shown within Figure 7 using a reference value of around 5 ns. It averages down with slope -1 [12]. On the other hand, the white frequency noise averages down with slope -1/2, which is shown as lower bound within Figure 7. It is based on the datasheet specification of the conducted rubidium clocks.
As a result of the measurement chain (time transfer technique), the observation noise dominates the observed Allan deviation of the clock relative to GPS time within the four stations. The white noise contribution can be extrapolated to be around 1 to 2 ns.
It is to be highlighted that in particular the accurate measurement of the time offset of each station clock relative to GPS time is of interest for the synchronization of the signals. As a consequence, it is focused by the campaign to determination the station and, thus, receiver dependent calibration values.
The used GNSS receiver models for stations A and B are Septentrio PolaRx2TR, for stations C and D PolaRx4TR. The difference in observed short term stability most likely originates from different tracking loop settings for those models. The long-term stability shows just minor differences.

B. Preliminary ranging results

As described above, by having knowledge about the clocks on ground and in the aircraft, true ranges between station A and the aircraft can be calculated. The root mean squared error (RMSE) for N measurements is

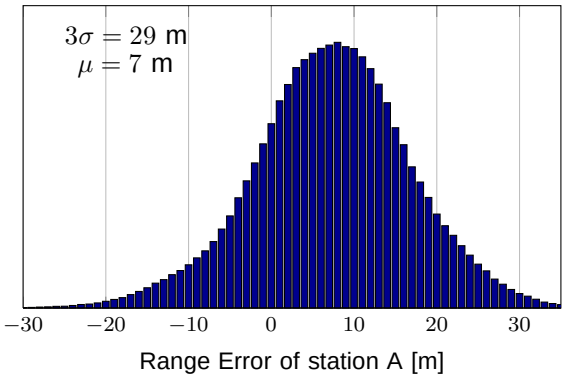

Figure 8: Error distribution for unprocessed ranges for a 100 s segment.

given as

$$\text{RMSE} = \sqrt{\frac{1}{N}\sum_{i=1}^{N} \mid \hat{\rho}_{i,\text{est}} - \hat{\rho}_{i,\text{ref}} \mid^2} \qquad (2)$$

with $\hat{\rho}_{i,\text{est}}$ and $\hat{\rho}_{i,\text{est}}$ being the i^{th} true range by the estimator and the GPS reference, respectively.

In Figure 8 the distribution of the range error in a 100 s segment is plotted. The ranges are unprocessed, i.e the output of the correlator is directly used and no post processing is applied. During the segment, the aircraft is flying at an elevation of 11 500 m and with a distance to the ground station of about 35 km. The high altitude minimizes the influences of multipath problems. The standard deviation is 9.6 m, that means $\approx 99.7\ \%$ (3σ) of the measurements are below 29 m. Compared to the usual accuracy of the system currently in use in civil aviation, the results are very promising. Nevertheless, a bias of 7 m still exists. The reason for that is currently being investigated. The overall RMSE is 12 m.

C. Preliminary positioning results

The barometric altimeter error is assumed to be Gaussian distributed with $N\left(0, \sigma^2 = 100\, m^2\right)$. Figure 9 shows the East-North error of the LDACS1 positioning solution compared to the reference GPS solution. The overall RMSE for this segment is 14.2 m. In the bottom of the figure we show the evolution of HDOP (Horizontal Dillution of Precision). The horizontal error appears as a combination of poor geometry and of ranging error. It has to be mentioned that the positioning solution is only generated using LDACS1 code measurements. A code smoothing with the phase would improve to a large extend the accuracy by reducing the impact of code multipath. Application of this method is subject of current research.

VI. Conclusion

In this paper, we described the setup and execution of a complex measurement campaign, designed to evaluate navigation with the aeronautical communication system LDACS1. Hereby, the synchronization of the different

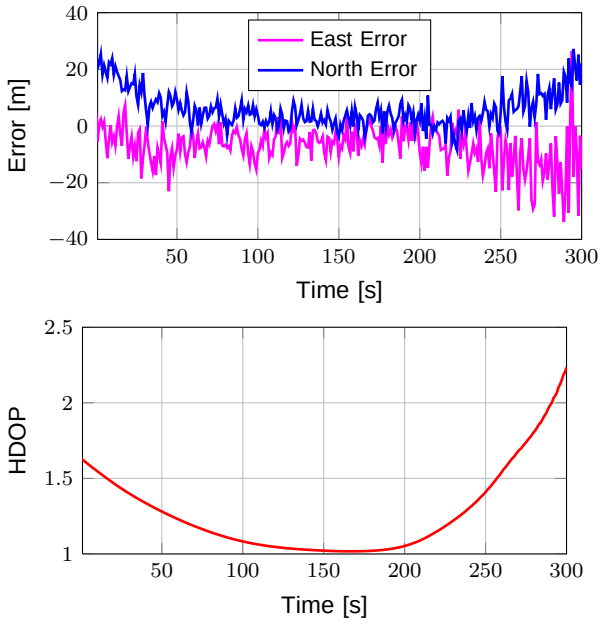

Figure 9: East-North LDACS1 position deviations to GPS and HDOP vs. time.

ground stations plays a crucial role. Since the analysis of more than half a tera byte of data has just been started, only preliminary results exist. These results are expected to be improved in the future. For the synchronization of the ground stations, a calibrated time transfer technique at each station was utilized to mitigate any hardware delays (biases) by the measurement equipment. The preliminary ranging results look very promising. Using unprocessed ranges, i.e. with no filtering or averaging being applied, a RMSE of less than 12 m is achieved. Assuming the aircraft being within the measurement area, and therefore having a good geometry, results for the horizontal position solution exhibit an RMSE of less than 15 m. Compared to the systems currently in use in civil aviation, these first results are already of a very high accuracy.

Nevertheless, several challenges are still to be addressed in future research. Of high interest is a quantitative assessment of all the error sources present in the measurement setup and their influence on the position error. This includes errors caused by the clock synchronization, unknown transmitter delays, inaccurate antenna positions or tropospheric delays along with aspects of the position geometry. Alternative synchronization methods are still under investigation [13]. In the field of range calculation, two issues are of special interest. Firstly, the resolution of multiple propagation paths. Although this problem does not arise often, it has to be addressed. Currently an improved version of the space-alternating generalized expectation-maximization (SAGE) algorithm is applied to the data to investigate the influence of multipath [14]. The first results look very promising. Secondly, interference by onboard equipment has to be mitigated. Currently, methods using pulse blanking techniques are

evaluated [15]. The range results are expected to be strongly improved by exploiting temporal correlations, e.g. a Kalman-filter using motion dynamics of the aircraft [11]. This will have a direct influence on the positioning performance.

ACKNOWLEDGMENT

The authors would like to thank the entire Institute of Communication and Navigation and the Institute of Flight Experiments for their continuous help, support and guidance. The authors are especially grateful for the great work of Michael Walter, Christian Hauswurz, Werner Rox, Martin Hammer, Hong Quy Le, Hazem Elsayed, Uwe-Carsten Fiebig, and Christoph Günther. Special thanks go to the staff at the 'Observatorium Hohenpeissenberg' of the German weather service (DWD), especially to Fritz Schönenborn, Claudia Unterreiner in Marktoberdorf, and Günter Schmid from 'Flugplatz Bad Wörishofen'. Without their support the setup of the ground stations would have not been possible. Thanks also go to TimeTech GmbH, Stuttgart, for their rapid provision of measurement equipment and Rücker Aerospace GmbH, Oberpfaffenhofen, for their support during the aircraft certification process.

REFERENCES

[1] J. Grabowski, 'Massive GPS Jamming Attack by North Korea', GPS Week, April 2012

[2] 'Personal Privacy Jammers: Locating Jersey PPDs Jamming GBAS Safety-of-Life Signals', GPS Week, May 2012

[3] C. Mensing et al., 'Data-Aided Location Estimation in Cellular OFDM Communications Systems', IEEE GLOBECOM, 2009

[4] M. Schnell et al., 'Using the Future L-band Communication System for Navigation', Integrated Communications, Navigation and Surveilance Conference (ICNS), 2012

[5] N. Schneckenburger et al., 'Precise Aeronautical Ground Based Navigation Using LDACS1', Integrated Communications, Navigation and Surveilance Conference (ICNS), 2012

[6] M. Sajatovic, B. Haindl, M. Ehammer, T. Gräupl, M. Schnell, U. Epple, and S. Brandes, 'LDACS1 System Definition Proposal: Deliverable D2', Eurocontrol Study Report, 2009

[7] P. Defraignea and G. Petit, 'Time Transfer to TAI Using Geodetic Receivers', Metrologia 40, p. 184-188

[8] B. Elwischger et al., 'Absolute Calibration of Dual Frequency Timing Receivers for Galileo', European Navigation Conference (ENC), 2013

[9] S. Thoelert et. al, 'Absolute Calibration of Time Receivers with DLR's GPS/Galileo HW Simulator', 39th Annual Precise Time and Time Interval (PTTI), 2007

[10] D. Allan and M. Weiss, 'Accurate Time and Frequency Transfer during Common-View of a GPS Satellite', Proc. 34th Ann. Freq. Control Symposium, May 1980

[11] S. Kay, 'Fundamentals of Statistical Signal Processing - Estimation Theory', Prentice Hall, 1993

[12] D. W. Allan, 'Time and Frequency (Time-Domain) Characterziation, Estimation and Prediction of Precision Clocks and Oscillators', IEEE Transactions on Ultrasonics, Ferroelectris and Frequency Control, Volumne UFFC-34, Number 6, p. 647-654, 1987

[13] M. Suess, B. Belabbas, J. Furthner, and M. Meurer, 'Robust Time Synchronization Methods for Future APNT', ION GNSS 2013

[14] D. Shutin and B. H. Fleury, 'Sparse Variational Bayesian SAGE Algorithm with Application to the Estimation of Multipath Wireless Channels', IEEE Transactions on Signal Processing, vol. 59, 2011

[15] U. Epple and M. Schnell, 'Overview of Interference Situation and Mitigation Techniques for LDACS1', Integrated Communications, Navigation and Surveilance Conference (ICNS), 2011